Magnetic Deflection Method for Angular Distribution of Electrons Scattered by Gas Molecules

A. PHARO GAGGE, *Sloane Physics Laboratory, Yale University*

(Received June 21, 1933)

A method is given for evaluating the scattering coefficient for electrons colliding with gas molecules, if the electrons both before and after collision describe circular paths in a uniform magnetic field. As in previous methods an electron gun and a receiver are needed. The axis about which the gun may be rotated is parallel to the receiver slits and lies some distance from their common plane on a perpendicular thereto through the center of the first slit. The second slit with Faraday collector can be set at such distances from the first slit as to collect only electrons that have lost a definite energy on collision. The chief advantage over previous methods used for angular distribution study is that, since all electronic paths are circular, the angular distribution may be studied up to 180° scattering angle. The fact that the collector may be set for electrons of definite energy allows both elastic and inelastic collisions of slow electrons to be studied. Typical experimental curves are given which show the variation with angle of the scattering coefficient in mercury vapor for 80 and 30 volt electrons. The scattering angles cover the range from 20° to 180°. These results are compared with those of previous observers over that portion of this range which they studied. An application of the method to the inelastic collisions of 23 volt-electrons in mercury vapor is included.

INTRODUCTION

AN inherent difficulty of the Dymond method[1] for the study of electron scattering by gas molecules is that the angular distribution of the scattered electrons cannot be studied up to 180°. The same is true for the zone method of Ramsauer and Kollath.[2] If the paths of the electrons are made circular before and after collision, by placing a uniform magnetic field perpendicular to the incident electron beam it is possible to devise an apparatus free from this limitation. The magnetic field in addition sorts the scattered electrons in accordance with their energies so that groups losing definite energies may be examined separately.

THEORY OF METHOD

As in Dymond's method a gun and a receiver are needed. The electron beam from the gun has a radius of curvature dependent upon the electron energy and magnetic field strength. If the pressure of the gas uniformly distributed throughout the apparatus is small enough to make multiple collisions unlikely, each volume element within the beam acts as a source of scattered electrons. The receiver slits in turn define a beam within which scattered electrons must move in order to be collected. The region common to both beams is that in which effective collisions occur. The general principle of the theory to be given is true for any receiver slit arrangement in which the four slit edges are parallel, but on account of its geometrical simplicity the arrangement to be considered in detail is that in which the parallel slits of the receiver lie in the same plane. This arrangement is similar to that used by Danysz in the β-ray spectrometer.

The essential geometry of the problem is illustrated in Fig. 1 (A, B). To pass through the collector slits S_1 and S_2 the centers of curvature of the electron paths must lie in the small region $ABCD$, formed by arcs of radius, R, whose centers lie at the slit edges. The electrons must enter upon these paths somewhere within the roughly circular area outlined (scattering area). At any point in this area, say P, the tolerance in angle (in the plane of the paper) which permits the scattered electron to reach the Faraday box is MN/R. The *average* tolerance for a given angular position, σ, of P (but varying

[1] E. G. Dymond, Phys. Rev. **29**, 433–441 (1927).

[2] C. Ramsauer and R. Kollath, Ann. d. Physik [5] **12**, 529–561 (1932).

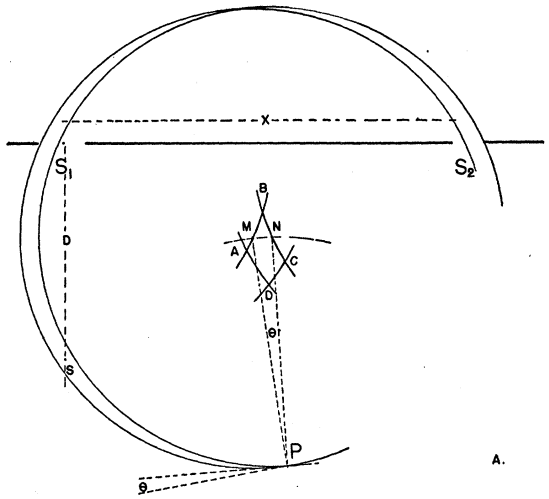

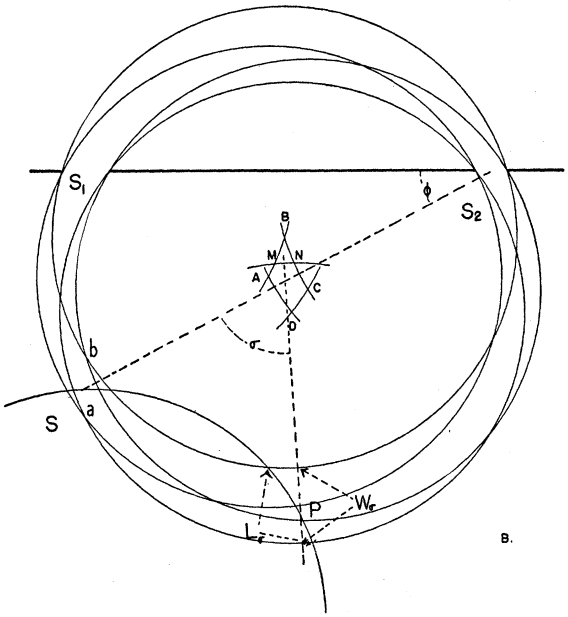

FIG. 1. Diagram of paths in a plane normal to magnetic field.

position of P across the scattering region) is

$$\bar{\theta}=(\text{area } ABCD)/RW_\sigma,$$

where W_σ is the radial distance across the scattering region at the angular position, σ.

The average tolerance in angle α with respect to the plane of the paper is (see Fig. 2a)

$$\bar{\alpha}=h/(\sigma+\pi)R,$$

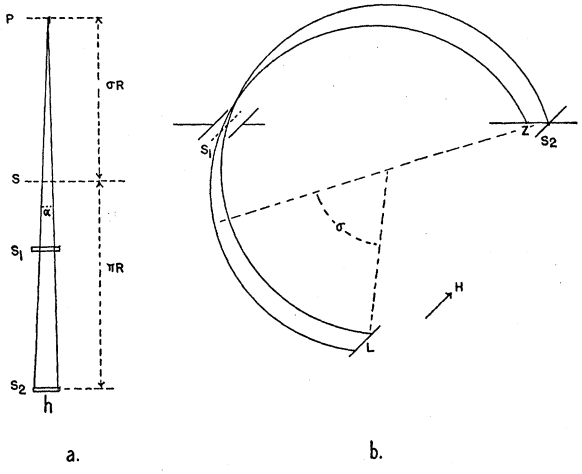

FIG. 2. Paths that do not lie in plane normal to magnetic field.

where h is the length of the slit S_2 and $(\sigma+\pi)R$ is the length of path of the electron. Strictly speaking the electrons scattered away from the plane of the diagram (see Fig. 2b) will have to have a slightly higher average energy to pass through the slit S_2 than do those moving in the plane. For the dimensions of the slits here used this fact need not be taken into account.

Hence the average solid angle $\bar{\omega}$ of the collected beam from P is, from (1) and (2),

$$\bar{\omega}=\bar{\alpha}\bar{\theta}=(\text{area } ABCD)\cdot\frac{h}{(\sigma+\pi)R^2}\cdot\frac{1}{W_\sigma}. \quad (1)$$

For small slit widths the area $ABCD$ is $s_1s_2x/2D$ where x is the distance between the centers of S_1 and S_2 and $D=(4R^2-x^2)^{\frac{1}{2}}$.

The point, S, in Fig. 1B lies at a distance, D, below the center of slit S_1. The incident beam is rotated about an axis through S. If θ is now the angle the incident beam makes with the direction of the scattered beam at S, it may be seen that the incident beam again crosses the collectable area at P. The point, S, is called the primary scattering region, while P is called the secondary scattering region. There will be a θ-value (in the case of the apparatus to be described, 95°) where, as θ is decreased, the initial beam strikes the walls of the receiver, and thus the secondary scattering region vanishes. For S the angle σ is always zero, while for P it

is variable and in no case greater than 80° for this particular arrangement.

The current collected *for a given pressure is*

$$I_\theta = I \cdot (\bar{\omega}_\theta \cdot L_\theta) \cdot S(\theta), \tag{2}$$

where I_θ is the collected current, I the initial beam at S, $\bar{\omega}_\theta$ the average solid angle, L_θ the path length, and $S(\theta)$ the so-called scattering coefficient, which is defined as the scattered current at $\theta°$ to the initial beam, per unit electron current, per unit solid angle, per unit path length.

The path length, L_θ, consists of two parts, L_0, due to the primary scattering region, and L_σ, due to the secondary region. The $\bar{\omega}_0$ (with $\sigma=0$) and $\bar{\omega}_\sigma$ are given by (1), and therefore

$$\bar{\omega}_\theta \cdot L_\theta = \frac{s_1 s_2 h \chi}{2\pi D R^2} [L_0/W_0 + L_\sigma \pi / W_\sigma (\pi+\sigma)]. \tag{3}$$

From (2) and (3)

$$I_\theta = I \frac{s_1 s_2 h \chi}{2\pi D R^2} [L_0/W_0 + L_\sigma \pi / W_\sigma (\pi+\sigma)] S(\theta). \tag{4}$$

For the apparatus here used $0° < \sigma < 80°$. In general, if R_i is the path radius of the initial beam and, as before, R, the radius of scattered beam, the relation between θ and σ is found to be

$$R_i \sin(\pi-\theta) = R \sin\sigma \cdot (R_i > R). \tag{5}$$

For the "elastic" case when $R_i = R$, $\pi - \theta = \sigma$. The bracketed term in Eq. (9) is called the "dispersion factor." For the Dymond method the equation corresponding to (9) is of the form

$$I_\theta = I \cdot S(\theta) \cdot K \cdot \csc\theta,$$

where K includes the dimensions of the apparatus. In that case the dispersion factor is $\csc\theta$.

The dispersion factor is determined graphically. From 10° to 140° the uncertainty of determination is easily reduced to 5 percent. From 140° to 170° the uncertainty increases to 10 percent on account of the greater range in the values of ω to be averaged. At 180° the uncertainty reduces again to 5 percent. A typical set of factor values is presented in Table II.

The graphical solution is carried out for inelastic collisions in the same way as for elastic collisions except that the more general value of σ in terms of θ given by Eq. (5) is used.

Apparatus

The general plan of the scattering chamber is shown in Fig. 3. The tube is a copper elbow to which the end plates are waxed with picein. The magnetic field from Helmholtz coils is perpen-

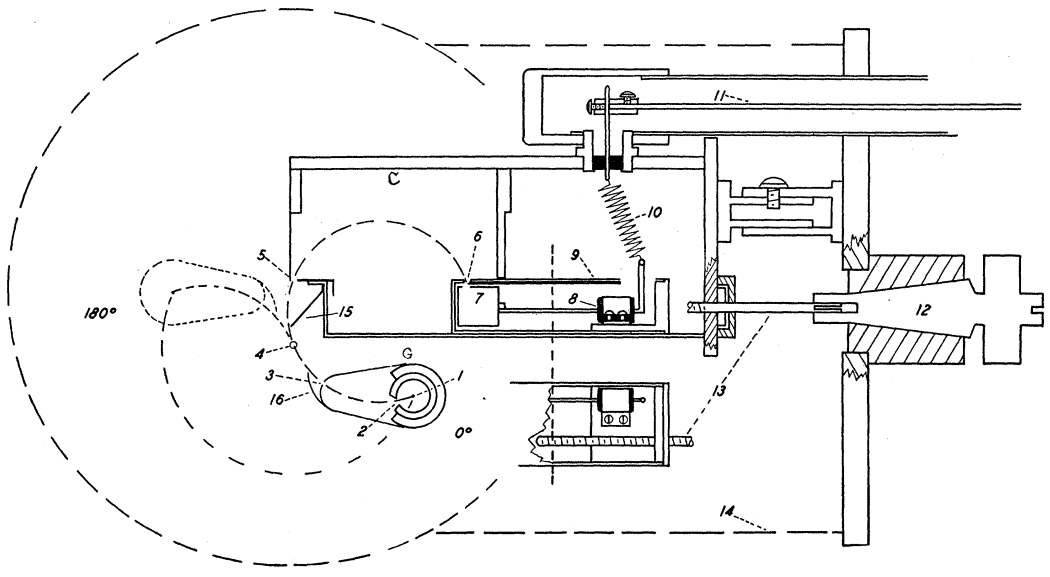

Fig. 3. General arrangement of apparatus.

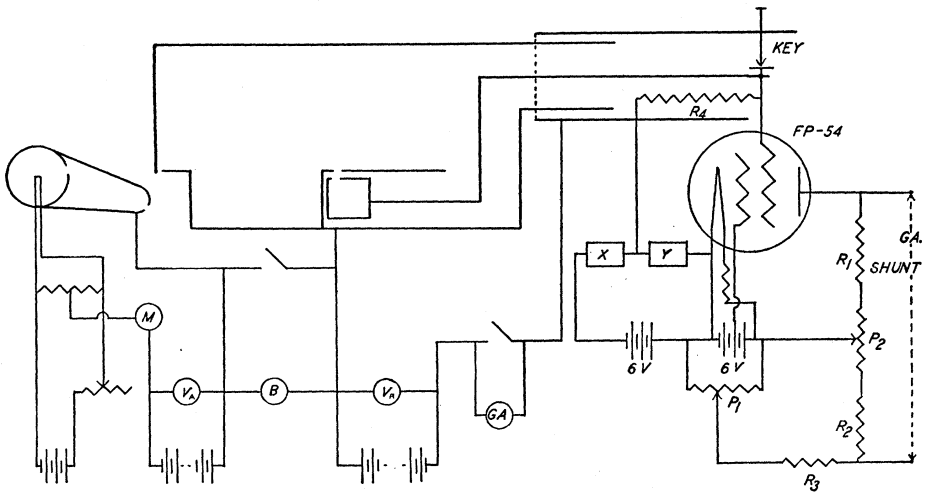

FIG. 4. Wiring diagram: M, microammeter; V_A, voltmeter for accelerating potential; V_R, voltmeter for retarding potential; B and GA, galvanometers; X and Y, resistances of constant sum 10,000Ω; R_1 and R_2, 10,000Ω; R_4, 20,000Ω; R_4, S. S. White Dental Co. high resistance of 10^{10}Ω; P_1 and P_2, 400Ω potentiometers.

dicular to the plane of the figure and deflects electrons from the gun into circular paths. This gun is mounted to rotate about an axis through a point (4) (the primary scattering region). Below the second defining slit (6) is the Faraday collector (7) which is connected to a vacuum tube electrometer. The gun is shown in two positions; at 0° where the primary beam passes directly into the collector and at 180° (dotted lines) where electrons scattered at (4) through 180° pass into the collector. The points (4), (5) and (6) define the path radius of the electrons collected. The slit (6) and Faraday box are mounted in a movable drawer (9) whose position is accurately controlled by a micrometer screw (13). In this way scattered electrons of various energies may be collected. The whole gun system is insulated from the receiver system by very thin washers of mica. A baffle (15) prevents the secondary electrons scattered by the lower step of the receiver from entering slit (5). A baffle (16) similarly protects the receiver from secondary electrons from the inner side of slit (3). (See Table I.)

TABLE I. *Dimensions here used (see Fig. 3).*

Slit (2)	1. mm×8 mm
Slit (3)	0.5 mm×4 mm
Slit (5)	1. mm (s_1)×10 mm
Slit (6)	0.4 mm (s_2)×10 mm (h)
Average radius of "elastic" circle	2 cm (R)
Distance from slit (5) to axis (4)	1.27 cm (D)

ADJUSTMENT AND USE

Fig. 4 is the wiring diagram used. The voltage sensitivity of the vacuum tube electrometer may be determined by making small changes in the resistances of the X and Y plug boxes. The constancy of the high resistance R_4 is checked easily by grounding the Faraday cylinder to its surrounding case and using batteries V_R and galvanometer G_A.

After every disassembly the gun and receiver units are placed in a separate vacuum furnace and baked for four hours at a temperature of 400°C. These parts are sealed into the elbow immediately after removal from the furnace.

The adjustment of the magnetic field is complete when for a given field strength, H, and accelerating potential, V_A, the initial beam passes through the axis of rotation for all angular settings of the gun.* The adjustment of the gun and drawer positions is complete when the Faraday box is able to collect the full initial

* To facilitate this adjustment slit (2) is made wide enough to permit a considerable range of beam curvatures for a given setting of (1), (2) and (3).

beam for 0° position of gun. When both these conditions are realized, the radius of the electron path as determined by the drawer position,* x, should equal the value of the radius conditioned by field, H, and electron energy, V_A. The apparatus is now ready for elastic collision study.

Inelastic collisions may be studied in either of two ways. In the first way the gun is fixed at a definite θ (with proper i for a given V_A) and x is decreased. In this way one will find the elastic peak and also the inelastic peaks. Resetting the drawer at a peak position and rotating the gun the angular distribution for electrons of the selected energy may then be obtained. The second and simpler method is to calculate the position of the drawer for a given energy loss and with drawer so set to vary the angle of scattering. To get fair resolution as one varies x for any fixed θ the retarding potential between (6) and (7) is best adjusted to be two or three volts less than $V_A - V_C$, where V_C is the energy loss in collision. The value of θ for inelastic collisions must be corrected by adding the angle between the line (4)–(6) for the elastic and inelastic settings of (6).

The usual tests for correct operation are applicable here: (1) at very low gas pressures no scattered beams should be found; (2) the collected currents should vary linearly with pressure; (3) the collected currents should have the expected energies when retarding potentials are applied, and (4) the collected currents should vary directly with the current in the initial beam.

Calculations and Curves

The second column in Table II gives for the dimensions in Table I, the graphically determined "dispersion factor," when $R_i = R$ (elastic case). It is found that under these conditions, if one varies s_1, holding s_2 constant, the values in Table II are independent of s_1. The factors for extreme θ's, however, depend greatly on s_2. For the case where $s_2 = 1$ mm instead of 0.4 mm the maximum value at 180° becomes 7.9 while the minimum at about 90° remains unchanged.

In the third column of Table II are the corresponding values of csc θ, dispersion factor of Dymond method. The cosecant term of the Dymond method corrects only for the change in path length of the initial beam which contributes to the scattered current. The value of $\bar{\omega}$ is assumed to be constant for all angles of scattering. However near the limiting case at 180° and near 0° ω may vary widely within the scattering region, and, as yet, no one using this method for large angle scattering (above 165°) has derived a sufficiently accurate value of $\bar{\omega} \cdot L$ to justify his results. The new method gives lower values for $S(\theta)$ in the border region from 150°–172° than those previously reported.

Table II. *Dispersion factors.*

θ	Gagge $[L, W]$	Dymond csc θ	θ	Gagge $[L, W]$	Dymond 2 csc θ
10°	4.68	5.76	100°	1.72	2.04
15°	3.58	3.86	105°	1.80	2.08
20°	2.90	2.92	110°	1.94	2.12
25°	2.40	2.37	115°	2.00	2.20
30°	2.00	2.00	120°	2.18	2.30
35°	1.70	1.74	125°	2.30	2.44
40°	1.50	1.56	130°	2.45	2.62
45°	1.40	1.41	135°	2.60	2.82
50°	1.30	1.31	140°	2.90	3.12
55°	1.20	1.22	145°	3.35	3.48
60°	1.15	1.15	150°	3.90	4.00
65°	1.10	1.10	155°	4.70	4.74
70°	1.05	1.06	160°	6.10	5.84
75°	1.04	1.04	165°	7.7	7.72
80°	1.02	1.02	170°	9.3	11.52
85°	1.00	1.00	175°	10.3	22.94
90°	1.00	1.00	180°	10.6	∞
95°	1.00	1.00			

As an illustration of the results to be expected of the magnetic deflection method, curves are presented in Fig. 5 for elastic scattering in mercury at two electron energies as shown. These two curves are compared with the corresponding curves taken from the recent paper of Jordan and Brode.[3] For the 80 volt curves the two are adjusted to agree at 80°. For the 30 volt curves they are made to fit at 165° to show what disagreement results at smaller angles. It will be noted that the magnetic deflection method reveals a new maximum in the very large angle scattering for these energies.*

* Use is made of the condition $R = (D^2 + x^2)^{\frac{1}{2}}$, or (4), (5) and (6) form a right triangle.

[3] E. B. Jordan and R. B. Brode, Phys. Rev. **43**, 112–115 (1933). In this paper their 80 volt curve is compared with earlier data of Arnot[4] and Tate and Palmer.[5]

* Preliminary curves for scattering in helium and argon do not show any maxima near 180°.

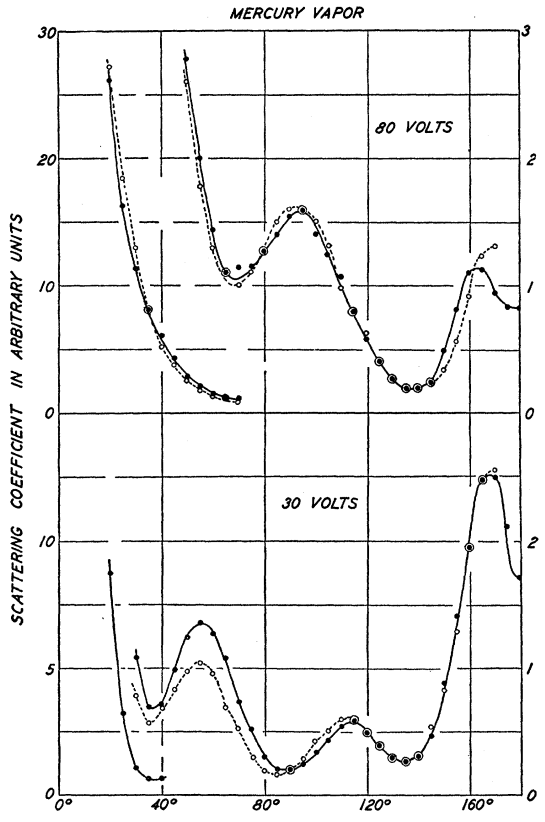

FIG. 5. $S(\theta)$ for 80 volt and 30 volt electrons. The ordinate scales of the two curves are unrelated. Circles, Jordan and Brode; black dots, Gagge.

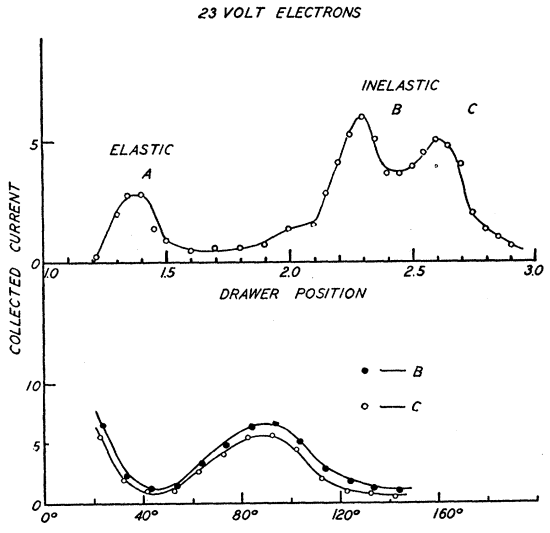

FIG. 6. Analysis of 23 volt electrons scattered in mercury vapor. B—4.9 volt loss $^1S_0-{}^3P_1$; C—6.7 volt loss $^1S_0-{}^1P_1$.

The course of $S(\theta)$ depends upon the values used for the "dispersion factors" (Fig. 5). The absolute values of the scattering coefficient depend also upon the remaining terms in Eq. (4). As an example, the value of $S(80°)$ for 80-volt electrons will be calculated. Using the following data in conjunction with Table I,

$$I_{80°} = -4.9\times10^{-14} \text{ amp.}$$
$$I_0 = -3.1\times10^{-7} \text{ amp.}$$
$$\text{pressure} = 1.2\times10^{-3} \text{ mm Hg}$$
$$\text{dispersion factor } 80° = 1.02,$$

one finds $S(80°)$ for 1 mm Hg to be 0.27. The absolute values found by other investigators for this particular point are

Jordan and Brode[3*]	0.14
Arnot[4]	0.43
Tate and Palmer[5]	1.00

This comparison emphasizes the difficulty of getting absolute values.

Fig. 6 gives some results for inelastic scattering in mercury vapor. In the top curve the gun is set at $\theta° = 80°$, and the collected current is plotted against the drawer position, x. In the lower curve by repeating this value for several values of θ the maximum currents for inelastic scattering are plotted against θ.

DISCUSSION

Certain limitations of the new method as here applied may be mentioned. The maximum electron-energy which can be studied depends on the maximum field the Helmholtz coils can produce. For the inelastic collisions the fractional loss of energy $(V_A - V_C/V_A)$ is the important factor. The smallest fractional loss that may be studied is 1/7. For small relative losses, x (inelastic) is nearly equal to x (elastic), and the inelastically scattered current may be increased by the presence of electrons of full energy. For fractional losses greater than three-quarters the method runs into geometrical limitations. Perhaps the most doubtful point is the graphical

* Inferred from a statement in their paper that their scattered currents were approximately one-third of Arnot's for similar initial conditions.

[4] F. L. Arnot, Proc. Roy. Soc. **A130**, 665–667 (1930–31).

[5] J. T. Tate and R. R. Palmer, Phys. Rev. **40**, 731–748 (1932).

calculation of the divergence factor in Eq. (9), but in the region from 15° to 150° results are easily as reliable as the corresponding values in the Dymond method. Between 150° and 170° the uncertainty increases but at 180° the graphical method is again as exact as in the 15° to 150° range. Therefore it is believed that values of $S(\theta)$ are significant in the whole range covered by the apparatus and are more reliable in the large angle range than those hitherto obtained by the Dymond method.

The method analyzes inelastically scattered electrons without appreciably altering their characteristics. In addition the system is ideally suitable for analyzing electrons of low energy without introducing an electrostatic accelerating or decelerating field near the supposed field free scattering region.

The author wishes to express his appreciation for the encouragement and generous advice given him throughout this work by Professor John Zeleny, and he is also indebted to Professor L. W. McKeehan for valuable suggestions in the design of the apparatus. Finally, the author is indebted to the Charles A. Coffin Foundation for a fellowship that made this work possible.